Quaternary Geochronology 82 (2024) 101545

Contents lists available at ScienceDirect

Quaternary Geochronology

journal homepage: www.elsevier.com/locate/quageo

Research paper

A luminescence dating study of the upper part of the loess-palaeosol sequence at kuldara, Khovaling Loess Plateau, Tajikistan

J.-P. Buylaert [a,*], A. Challier [a], E.P. Kulakova [b], N.A. Taratunina [a], K.J. Thomsen [a], A.O. Utkina [c], P.M. Sosin [d], O.A. Tokareva [e], A.A. Anoikin [f], T.U. Khujageldiev [b], C. Karayev A [b], N.K. Ubaydulloev [b], A.S. Murray [g], R.N. Kurbanov [d]

[a] Department of Physics, Technical University of Denmark, Denmark
[b] A. Donish Institute of History, Archaeology and Ethnography, National Academy of Sciences of Tajikistan, Tajikistan
[c] Research Center for Geochronology and Isotope Analysis, Korea Basic Science Institute, South Korea
[d] Institute of Water Resources, Hydropower and Ecology, National Academy of Sciences of Tajikistan, Tajikistan
[e] Gorgan University of Agricultural Sciences and Natural Resources, Gorgan, Iran
[f] National Museum of Kazakhstan, Astana, Kazakhstan
[g] Nordic Laboratory for Luminescence Dating, Aarhus University and Department of Physics, Technical University of Denmark, Denmark

ARTICLE INFO

Keywords:
OSL
Loess-palaeosol sequences
Hiatus
Dust accumulation rate
Aeolian dust
Tajikistan
Late Quaternary
Central Asia

ABSTRACT

The aim of this study was to develop an independent luminescence chronology for the upper part of the important Loess Palaeolithic site at Kuldara (Khovaling Loess Plateau, Tajikistan). We applied high sampling-depth resolution (n = 85) luminescence dating to the upper ~26 m of the sequence from loess L4 to pedocomplex PC0. Luminescence characteristics of the post-IR_{200} $IRSL_{290}$ signal from coarse-silt polymineral grains are satisfactory (reproducible growth and good dose recovery). Comparison with quartz OSL for samples <50 ka and results from modern analogues (Challier et al. these proceedings) shows that the $pIRIR_{200,290}$ signal is, as expected, sufficiently bleached at deposition. The luminescence chronology extends back to ~250 ka and shows distinct erosional hiatuses ranging in duration from ~15 ka to a full glacial-interglacial cycle (~100 ka); some of these breaks were not identifiable in the field. We suggest an upper dating limit of $2.5xD_c$; this yields minimum ages of ~300 ka for this material. Dust Accumulation Rates (DAR) are reconstructed for the Late Pleistocene (from ~100 to ~40 ka) and reveal, next to several minor dust accumulation peaks, two major peaks at the end of MIS5 (~75 ka) and at MIS3b (~40 ka). We conclude that detailed post-IR_{200} $IRSL_{290}$ dating of loess-palaeosol sequences in Tajikistan is necessary to exploit fully the potential of this important terrestrial (dust) record.

1. Introduction

In Central Asia the high sensitivity of landscapes to climate change was manifested in the formation of thick loess-palaeosol series (LPS), forming a continuous cover from the southern slopes of the Kopetdag mountains in the west to the foothills of the ranges of Pamirs, Altai and Tien Shan in the east. During interglacial periods, a series of polygenetic palaeosols were formed here, sometimes separated by thin loess layers, which together form pedocomplexes (PC). The pedocomplexes may contain from one to three-four palaeosols, but correspond to one interglacial. During the dry and cold conditions of glacial times, thick layers of loess were deposited. The duration of one loess-palaeosol cycle in the Middle Pleistocene was estimated at ~100 ka (Dodonov, 2007). In this region the large masses of atmospheric dust were accumulating due to input from various sources: local rivers, glacial tills and slope sediments of the near-by mountains (Pamirs and Hindukush) and the vast sandy deserts of Central Asia (Karakum, Kyzylkum, Betbak-Dala and others).

The most complete sections of the LPS, with a thickness up to 200 m, are found in Southern Tajikistan, where complex studies of a series of natural outcrops were carried out within the Khovaling Loess Plateau in the second half of the 20th century. A unique feature of the sections in Khovaling is the high detail of the Quaternary sedimentary record (contains up to 40 PCs) and significant chronological coverage (more than 2.1 Ma, Parviz et al., 2020). The LPS of Southern Tajikistan were intensively studied as a basis for the development of a detailed Pleistocene stratigraphic chart for the entire Central Asian region (Dodonov,

* Corresponding author.
E-mail address: jabu@dtu.dk (J.-P. Buylaert).

https://doi.org/10.1016/j.quageo.2024.101545
Received 15 November 2023; Received in revised form 3 May 2024; Accepted 14 May 2024
Available online 17 May 2024

2002; Ding et al., 2002).

In addition to the obvious palaeogeographical and stratigraphic significance, the LPS of southern Tajikistan contain several horizons containing Palaeolithic artefacts. Within the region, a series of Early and Middle Palaeolithic sites were discovered, which allowed the prominent Soviet-Tajik archaeologist V.A. Ranov to develop the concept of the "loess Palaeolithic" (Ranov, 1995; Ranov and Schaefer, 2000). With this term he designated the stone industries of the Early and Middle Paleolithic occurring in loess and palaeosols. Typical industries of the "loess Paleolithic" (LPal), found at several sites in Southern Tajikistan, were discovered by V.A. Ranov in the 70s of the 20th century (Ranov, 1995; Ranov and Schaefer, 2000; Ranov and Karimova, 2005). At present, archaeological studies of the LPal in Tajikistan have shown the presence of three main stages in the development of hominins and their material culture in Central Asia. The following stages are distinguished: (i) the earliest, associated with PC's 11 and 12 at the Kuldara site (Ranov et al., 1987) is estimated at ~800–900 ka; (ii) a subsequent stage that recorded when a developed pebble-tool Early Palaeolithic industry formed in the region - the so-called Karatau culture of Central Asia, prominent in PC's 6–4 at a number of sites (Anoikin et al., 2023a); and (iii) the stage associated with the Middle Palaeolithic cultures that occur in PCs 2 and 1 (Ranov, 1995; Anoikin et al., 2023b).

From the above, it is clear that the Kuldara site is a very important site to study the Loess Palaeolithic of Tajikistan. The chronology of the site has been built on the correlation of loess and palaeosol horizons with the global marine isotope stage (MIS) record and on palaeomagnetic data, which showed the presence of the Brunhes/Matuyama boundary in the loess horizon L10 (between PCs 9 and 10), recently clarified by us at the base of PC9 (Kulakova and Kurbanov, 2023). This allowed the discoverer of the site, V.A. Ranov to determine the age of the artefact bearing layers to be ~0.9–0.8 Ma (Ranov et al., 1987). Dodonov (2002) described the stratigraphy at Kuldara but his work only starts from PC4 down. However, the first approach, associated with the numbering of the PCs and their correlation with MIS, often does not take into account the possible incompleteness of the geological record in loess sections, and possible long-term hiatuses. In recent years, the use of detailed luminescence dating has shown the presence of such breaks in LPS in different regions of the world from China (Stevens et al., 2018) and Siberia (Volvakh et al., 2022) to Eastern Europe (e.g., Murray et al., 2014; Thiel et al., 2014). In Tajikistan, Frechen and Dodonov (1998) performed relatively high resolution IRSL and TL dating of the Darai Kalon section but they were only able to independently constrain the age of the upper pedocomplex (PC1) to the last interglacial period. Current (MET)-pIRIR methodology should in principle allow us to develop independent chronologies back to ~250 ka (e.g., Li and Li, 2011; Stevens et al., 2018) and this is the approach taken in this study.

As part of the international THOCA (The Timing and Ecology of the Human Occupation of Central Asia, www.thoca.org) project, we carried out a comprehensive study of a section at Kuldara site to clarify mainly the upper part of the stratigraphic scheme and to constrain the age of the

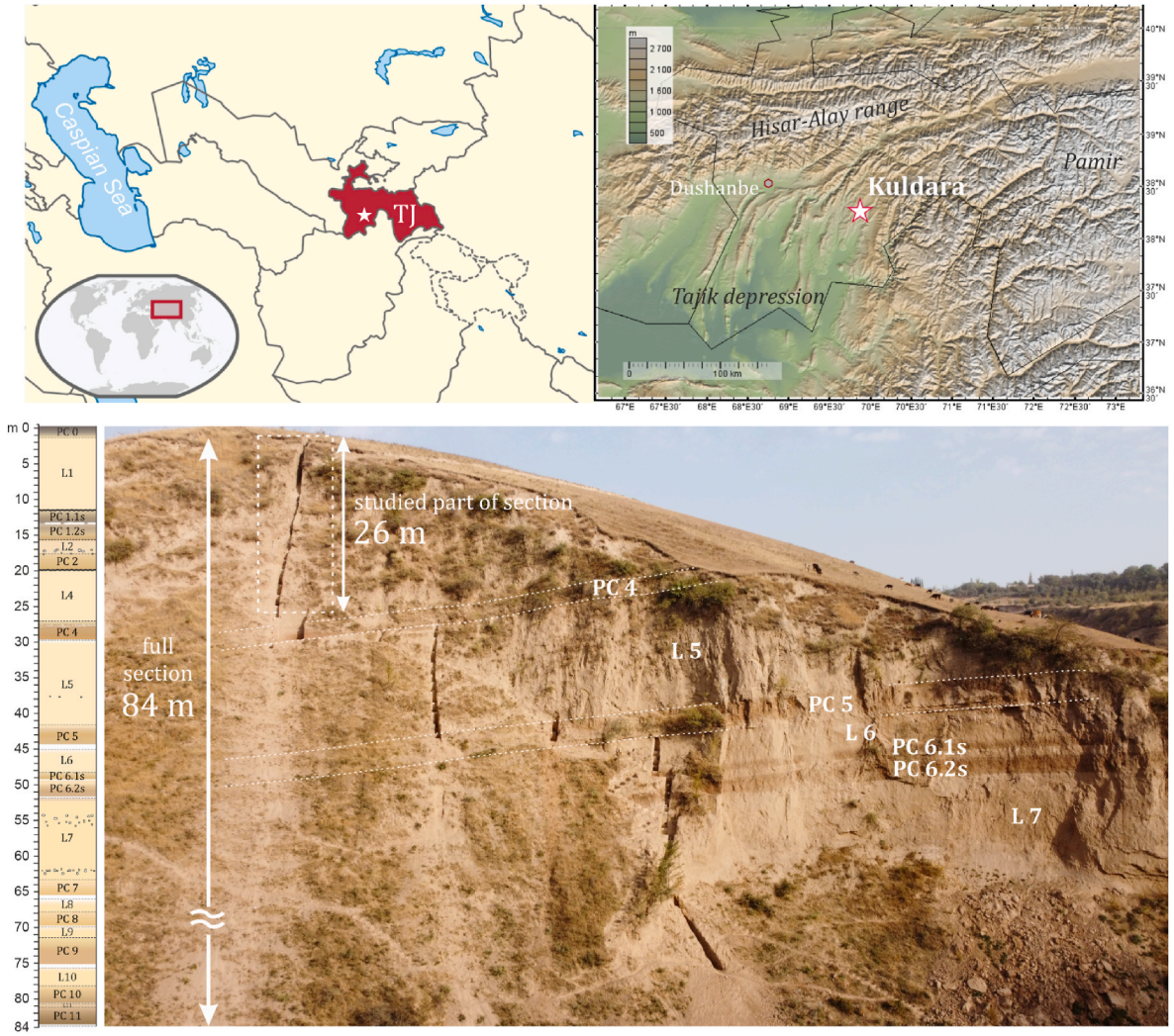

Fig. 1. Location of the Kuldara section, its general view and stratigraphic column.

(upper) palaeosols. We specifically revisited the same location that Ranov studied so that our findings can be directly related to the earlier published results (Ranov et al., 1987). We develop the first high-resolution luminescence chronology at Kuldara with the main aim of checking the completeness of upper part of the LPS record and to study the main stages of dust accumulation over this interval.

2. Study area and site description

The Loess Palaeolithic site of Kuldara (N 38.28277°, E 69.88564°) is located within the Khovaling Loess Plateau in Southern Tajikistan (Fig. 1), in a Kuldara gully ~1.8 km south of the group of other LPal sites - the Obi-Mazar, Lakhuti-I and Lakhuti-IV sections (Anoikin et al., 2023a). The Kuldara gully is a left tributary of the Obi-Mazar River, with a length of ~5–6 km. The gully was formed by a watercourse, currently in the form of a small stream fed by a series of springs. The height of the outcrops of loess walls in some areas reaches 70–80 m and visibly includes up to 15 PCs.

To create a detailed stratigraphic chart of the section and to obtain data on the absolute ages for the sediments, a series of geological trenches were prepared on the right bank of the Kuldara gully revealing a steep loess wall. To characterize the complete structure of the LPS, sediments from the presumed Holocene soil (PC0) to PC 11, with a total thickness of 84 m, were exposed (Fig. 1). Within a pedocomplex individual palaeosols are numbered from top to bottom 1.1s, 1.2s, 1.3s., etc.

3. Methodology

3.1. Fieldwork and sampling

During the expeditions in 2021 and 2022 the outcrop was opened in a series of trenches; the trenches were correlated with each other using marking calcite horizons at the base of the developed PCs. We described the structure of the sediments and soil characteristics and measured field magnetic susceptibility using a portable Kappameter continuously over the entire length of the studied profile. Eighty-five luminescence samples were taken by hammering 5 cm diameter, ~25 cm long stainless-steel tubes into freshly cleaned sediment surfaces down to a depth of 25.8 m. Between 0 and 10 m the sampling interval was 15–20 cm, between 10 and 18 m the interval was increased to 30–60 cm and the lower 7 m of the section sampled approximately every ~1 m.

3.2. Dose rate: preparation, measurement and calculation

Luminescence samples were opened under subdued orange light conditions (Sohbati et al., 2017) at the Donish Institute of History, Archaeology and Ethnography in Dushanbe (Tajikistan). Both the outer ~5 cm and the inner tube material were split in two; one half is kept in Dushanbe for backup and half was shipped to Denmark for further processing. The outer material was dried at 80 °C, homogenised by grinding using a ring-grinder and cast with wax in a cup (n = 77) or disc (n = 8) geometry to retain ^{222}Rn. The cups/discs were counted for ~24 h on a high-resolution gamma spectrometer following Murray et al. (1987, 2018) to provide concentration measurements of ^{238}U, ^{226}Ra, (^{210}Pb), ^{232}Th and ^{40}K.

Infinite matrix beta and gamma dose rates were calculated using the conversion factors from Cresswell et al. (2018); for the alpha dose rate calculation we used the emitted alpha energies tabulated in Guérin et al. (2012) and the ranges in SiO2 from https://physics.nist.gov/cgi-bin/Star/ap_table.pl in combination with equations 4.9 (p.84) and K.8 from Aitken (1985). For quartz OSL an a-value of 0.035 ±0 .003 was used (Lai et al., 2008) and for post-IR IRSL signals from polymineral grains we adopted a value of 0.09 ± 0.02 based on Schmidt et al. (2018). The cosmic ray contribution was calculated following Prescott and Hutton (1994).

For quartz, we assumed an internal dose rate coming from U, Th of 0.010 ± 0.005 Gy/ka based on Vandenberghe et al. (2008); the corresponding value for polymineral grains is 0.10 ± 0.05 Gy/ka (Zhao and Li, 2005). We assumed that the luminescence in our polymineral grains comes primarily from K-rich feldspar and to calculate the internal beta dose rate for a 50 μm grain we assumed a K concentration of 12.5 ± 0.5% and a Rb concentration of 400 ± 100 ppm (Huntley and Baril, 1997; Huntley and Hancock, 2001). For the calculation of the external alpha component to these polymineral grains we used an alpha attenuation factor of 0.40 ± 0.10 (Martin et al., 2014); for quartz, despite the same original grain size, we used a lower value of 0.30 ± 0.10 because we assume that some portion of the alpha-irradiated rind was removed by our concentrated HF treatment (see below section 3.3). For calculation of the wet dose rates the attenuation factors of Aitken (1985) were used; for the alpha dose rate component we further assumed that 50% of the alpha particles underwent attenuation by pore moisture and the remaining 50% (originating from grain coatings) did not.

Present day water content measurements on five samples taken from freshly cleaned exposures in units L1, L2, L4 and PC4 gave water contents in the range 15–17% (sections were dug several days earlier). These values are almost certainly minimum values because of the possible drying out of the section walls and because the profiles were made at the edge of a loess hill (ideally one would drill a core at the centre of a loess hill). Based on these arguments and in line with the water content model presented by Challier et al. (these proceedings) for S0 and L1 at Khonako II, we adopted a water content of 20 ± 4% and 25 ± 4% for the loess and pedocomplex units, respectively.

3.3. Luminescence: preparation, measurement, and dose calculation

Inner material was first treated with 10% HCl for 2–3 days to remove the majority of the carbonates and to disaggregate the sediment. This was followed by wet-sieving on large 304.8 mm diameter sieves of 38 and 63 μm mesh size. The 38–63 μm fraction was further treated with HCl (10%) again to make sure all carbonates were removed and then treated with H_2O_2 (10%) to remove organic material. The 38-63 μm fractions were repeatedly washed with deionised H_2O after the HCl and H_2O_2 steps. In order to extract a 38–63 μm quartz extraction a portion of this material was etched with concentrated HF for 15 min followed by washing with 10% HCl and H_2O_2 and final resieving on a 38 μm sieve. After drying at 50 °C, both the dried quartz and polymineral fractions were mounted as large (∅ = 8 mm) aliquots on stainless steel cups for luminescence measurements.

Luminescence measurements were undertaken on standard Risø TL/OSL readers equipped with a classic or DASH stimulation head (Bøtter-Jensen et al., 2003; Lapp et al., 2015) and calibrated ^{90}Sr/^{90}Y beta sources using Risø calibration quartz mounted on stainless steel cups (Hansen et al., 2018; Autzen et al., 2022). Quartz OSL signals, detected through a Hoya U-340 glass filter, were measured at 125 °C using blue-light stimulation (470 nm, >80 mW cm^{-2}) for 40 s using a double SAR protocol (Banerjee et al., 2001). An infra-red (IR) bleach at 60 °C for 100s preceded the blue light stimulation because most samples showed small but still detectable IRSL signals. A preheat/cut-heat combination of 240 °C/10s and 200 °C/0s was used and each SAR cycle ended with an elevated temperature (280 °C) blue-light stimulation for 40 s to minimise recuperation (Murray and Wintle, 2003). Early background subtraction (Cunningham and Wallinga, 2010) was employed for all dose calculations (signal: 0.0–0.8s, background: 0.80–1.60 s). Polymineral grains were measured using a SAR post-IR IRSL protocol (pIRIR$_{200,290}$). The pIRIR$_{200,290}$ signal from K-rich feldspar has been shown to be very stable (Li and Li, 2012; Yi et al., 2016) and has previously been successfully employed in many loess dating studies (e.g. Stevens et al., 2018; Volvakh et al., 2022). The duration of all IR stimulations, including the elevated temperature clean-out at 325 °C, was 200 s and net signals were calculated from the first 2 s of stimulation minus a background derived from the last 20 s of stimulation. IRSL signals were detected through a blue filter combination

(Schott BG3 and BG39 filters). All quartz OSL and polymineral $pIRIR_{200,290}$ dose response curves were fitted using the *Analyst* v4.57 software package (Duller, 2015). In the $pIRIR_{200,290}$ measurements, a test dose of 30–50% of the measured D_e was used (Yi et al., 2016). A single saturating exponential function adequately fitted the $pIRIR_{200,290}$ signals. For quartz OSL single saturating exponential functions were employed, or, more typically, a sum of two saturating exponential functions to ensure a good fit of the laboratory dose response curves.

3.4. Age-depth modelling

Bacon software (Blaauw and Christen, 2011) was used for age-depth modelling the part of the section that did not show any hiatuses (see below). Standard Bacon settings were used and uncertainties on the ages only contained the random component. Modelled ages were produced for every 5 cm.

4. Results

4.1. Field observations

In total seven stratigraphic units were distinguished (from top to bottom, Fig. 3a):

Unit I. 0–1.50 m. Layer 1. Modern dark gray, leached, heavily eroded soil (Hs). The transition is gradual.

Unit II. 1.50–11.53 m. Typical loess L1, yellow-beige. The transition to the PC below is sharp, along the erosional boundary (presumed hiatus 1).

Unit III. 11.53–15.60 m. Pedocomplex PC1, consisting of two developed palaeosols of dark brown colour with a gray tint. The transition is gradual.

Unit IV. 15.60–17.60 m. Loess L2, dark yellow. It can be classified as a transitional type to palaeosol (LB); abundant bioliths. At a depth of 16.73–17.18, a horizon with $CaCO_3$ nodules up to 10 cm stands out. The transition is gradual.

Unit V. 17.60–19.85 m. Pedocomplex PC2, in the form of one developed palaeosol. At the base there is a horizon of $CaCO_3$ concretions 2–4 cm thick. The transition to loess is sharp along a pronounced erosional boundary (presumed hiatus 2).

Unit VI. 19.85–27.05 m. Typical loess L4, beige. The transition is gradual.

Unit VII. 27.05–29.70 m. Pedocomplex, in the form of one thick dark brown palaeosol. Due to existence of the erosional boundary at the basis of Unit V and characteristic features of this monosoil pedocomplex we correlate this unit with PC4 of the regional stratigraphic chart of LPS of Tajikistan (there PC4 is also represented by one developed palaeosol) (Schäfer et al., 1998; Kulakova et al., 2024). At the base of the soil there is a whitish carbonate crust. The transition is abrupt.

4.2. Luminescence dating

4.2.1. Dosimetry

Radionuclide concentrations and dry infinite matrix beta, gamma and alpha dose rates are summarized in Table S1 and total quartz and feldspar dose rates are given in Table S2. The average $^{210}Pb/^{226}Ra$ ratio is 0.96 ± 0.02 ($n = 48$) indicating no Rn loss during burial and dose rates were calculated accordingly. It should be noted that the calculated external alpha dose rate component is small for both quartz and polymineral grains, ~0.14 Gy/ka and ~0.50 Gy/ka, respectively. The resulting total dose rates are typical for loess (~3–4 Gy/ka). The radionuclide concentrations and total feldspar dose rates are also plotted as a function of depth in Figs. S1a–d. In general, there is little variation as a function of depth but dose rates appear to peak between ~11 and ~13 m at the location of the PC1.1s palaeosol. This peak gradually returns to normal typical loess dose rates by ~9 m in the L1 loess above. Between ~13 m and ~17 m (PC1.2s, PC1.3 l and L2), the radionuclide concentrations and total dose rates display more variability.

4.2.2. Quartz and polymineral grains: luminescence characteristics

Fig. 2a shows a typical quartz OSL dose response and stimulation curve (inset) for sample 229120 (depth of 323 cm). Comparison of the natural decay curve with Risø calibration quartz shows that the quartz OSL signal is clearly dominated by the fast component (see also Challier et al. these proceedings). The dose response of this aliquot was well-represented by a single saturation exponential with a D_c value (Murray et al., 2021) of 64 Gy; the natural signal lies close to the upper dating limit of $2xD_c$ suggested by Wintle and Murray (2006). Quartz OSL dose response curves for samples with D_e values $\gtrsim$ 100 Gy typically required an additional saturating exponential function to fit the dose response adequately and this was also done here. A dose recovery test was carried out on three samples (229119, −22, −24) by adding ~30, ~60 and ~90 Gy to six blue LED bleached (2×100 s with a 10 ks pause in between) aliquots per sample per given dose. No clear trend could be observed in the dose recovery ratio and the overall measured to given dose ratio is 1.12 ± 0.02 ($n = 9$, 54 aliquots) which is only considered to be just acceptable (Fig. S2). It is interesting to note that analysis of the same data in terms of light level (Murray et al., 2021) the recovery ratio improves to 1.072 ± 0.010; this is a more satisfactory result. It appears that the curvature of the dose response plays a role and for testing the performance of a SAR protocol it may be interesting to also consider the light recovery ratio. Fifty out of eighty-five samples had a quartz OSL D_e measured and the results are summarized in Table S2.

Fig. 2b shows the average (3–6 aliquots/sample) sensitivity corrected $pIRIR_{200,290}$ L_x/T_x values (±s.e.) for polymineral 38–63 μm fractions from samples 229177, -78, −79 and −85; the L_n/T_n ratios (±s.e.) are also shown. As expected the dose response for these aliquots/samples is identical and the data is well-represented by a single saturating exponential with $D_c = 476$ Gy. The bottom two samples in PC2 (229177 and −78) have L_n/T_n values very close to 86% of the saturation level (dashed horizontal line) and thus their D_e values (892 ± 28 Gy and 922 ± 35 Gy, respectively) are close to $2xD_c$. A dose recovery test was also carried out using a SARA approach (Mejdahl and Bøtter-Jensen, 1994) on the top sample (229101) (Fig. 2c); for each dose point, the test dose was kept at ~30% of the measured dose. From the slope (1.051 ± 0.014) of the linear fit through the data we conclude that our $pIRIR_{200,290}$ protocol performs satisfactorily.

It is well-known that $pIRIR_{290}$ signals have a hard-to-bleach residual (Buylaert et al., 2012) that needs to be taken into account. Here we have subtracted a residual dose of 9.2 ± 0.4 Gy from the $pIRIR_{200,290}$ D_e values tabulated in Table S2; this value is adopted from Challier et al. (these proceedings) who derived it from the quartz OSL and $pIRIR_{200,290}$ results of three modern analogue samples and a set of samples from the top of L1 and Holocene soil of the nearby Khonako-II section.

In this study, we suggest to take $2.5xD_c$ (1190 Gy; ~92% saturation) as the upper limit for finite dose estimation; our highest finite D_e value (922 ± 35 Gy) is not $>2xD_c$. Samples with L_n/T_n values beyond this ~92% limit are quoted as minimum doses (Table S2). A significant increase (~10%) in L_n/T_n level can be observed from sample 229178 to sample 229179 even though the vertical sampling distance is only 30 cm larger than between samples 229177 and -78; this strongly suggests a missing part of the sediment sequence between samples from 229178 to -79. Samples 229179 and -85 have L_n/T_n values very close to saturation. It is interesting to interpolate the average L_n/T_n (±s.e.) values on the average dose response curve; this yields indistinguishable D_e values (with asymmetric uncertainties) of $1500\ ^{-285}_{+800}$ Gy for sample 229179 and $1202\ ^{-70}_{+78}$ Gy for sample 229185, the lowermost sample in this study.

4.2.3. Luminescence ages and bayesian age-depth model

In Fig. 2d we have plotted the $pIRIR_{200,290}$ ages as a function of the quartz OSL ages for the last 110 ka. There appears to be a fairly good agreement between ~35 and ~40 ka (typical quartz D_e range of

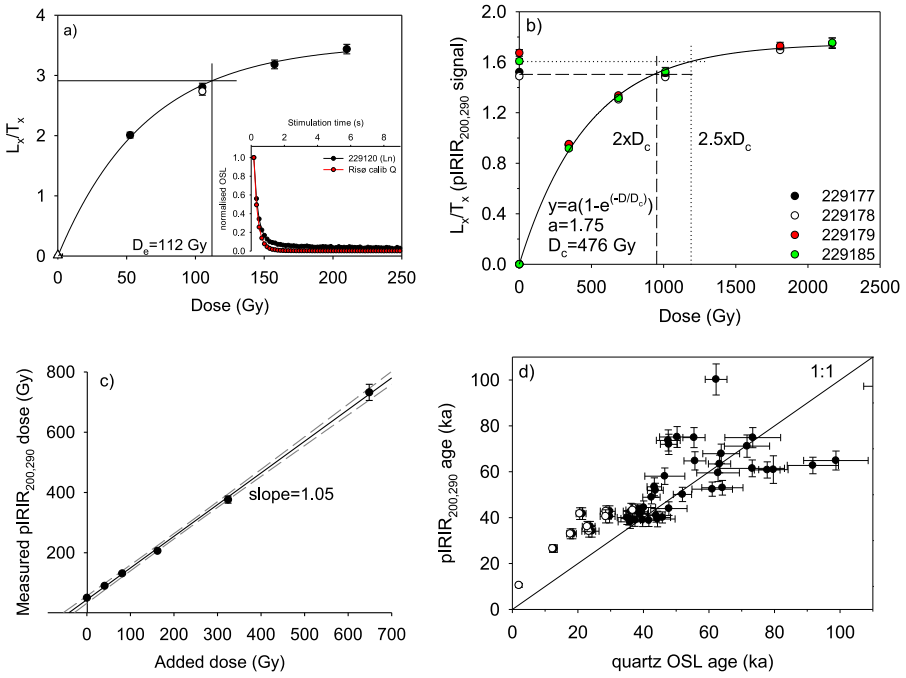

Fig. 2. Quartz OSL and polymineral $pIRIR_{200,290}$ luminescence characteristics and age comparison back to 110 ka. a) Dose response curve and decay curve for an aliquot from sample 229120. Recycling and recuperation points are shown as open circle and triangle, respectively. Inset shows normalized natural (black) and calibration quartz (red) decay curves. b) Average $pIRIR_{200,290}$ dose response (L_x/T_x) measured for 4 samples (3–6 aliquots/sample) using a test dose of 343 Gy. Dashed and dotted lines show interpolation at 2xD_c and 2.5xD_c, respectively (corresponding to 86% and 92% of saturation level, respectively). c) $pIRIR_{200,290}$ SARA dose recovery test using sample 229101; test dose was kept at 30% of measured doses; error envelope shown at 1 sigma. d) $pIRIR_{200,290}$ ages plotted as a function of their quartz OSL ages for the last 110 ka; open circles refer to the nine samples 229101–09 from the upper 1.5 m in PC0.

~100–150 Gy) but for older samples the scatter increases quite pronouncedly. Fig. S3 shows both quartz and polymineral ages as a function of depth and it can be seen that the increase in scatter is because of increased scatter in the quartz OSL ages. There is also a tendency for the quartz ages to begin to underestimate the $pIRIR_{200,290}$ ages beyond ~40 ka although some are in fairly good agreement. Many studies have shown that quartz OSL age in loess beyond ~40–50 ka (typically ~150 Gy) are often problematic probably due to saturation effects and/or mismatch between natural and laboratory dose response curves (Buylaert et al., 2007; Chapot et al., 2012; Timar-Gabor and Wintle, 2013). For the upper samples taken in the presumed modern soil (PC0; open circles in Figs. 2d and 229101–09) the $pIRIR_{200,290}$ ages clearly overestimate the quartz OSL ages. We attribute this to recent pedogenic or colluvial disturbance that has caused a differential bleaching between the readily bleachable quartz OSL signal and the much harder to bleach $pIRIR_{200,290}$ signal. The $pIRIR_{290}$ ages probably reflect the timing of deposition of the loess whereas the quartz OSL ages would be closer to the latest timing of soil turbation or colluvial processes. We cannot be certain that the $pIRIR_{200,290}$ ages have not been affected by these processes and underestimate the true deposition age to some unknown degree. Nevertheless, it is clear from the $pIRIR_{200,290}$ ages that the top part of the section is missing because no sediment with $pIRIR_{200,290}$ ages <30 ka are present; the material making up PC0 was not deposited during the Holocene but rather during MIS3. Because the problems associated with quartz OSL at high doses and the pedogenic disturbance of the PC0, we decided to focus our efforts on measuring all the samples using the $pIRIR_{200,290}$ signal and to use these ages for age modelling and subsequent interpretation (see Discussion below).

It is interesting to note that the apparent dose rate scatter between ~13 m and 17.5 m depth (Fig. S1d) is compensated almost entirely by the measured $pIRIR_{200,290}$ D_e values (Fig. S1e) so that the age-depth relationship is almost free of inversions (Fig. S1f). This suggests that the dose rate changes are real and not induced by post-depositional processes.

The $pIRIR_{200,290}$ ages are shown in Fig. 3b together with a Bayesian age-depth model obtained on seventy-two samples (229102 to −73). The top sample (229101) was discarded because it is clearly affected by recent processes and we chose to limit our Bayesian model to a depth of 1687 cm (sample 229173) because we suspect a hiatus between samples 229173 and -74 (see Figs. S1f and S3, Table S2 and Discussion below).

4.2.4. *Dust accumulation rate*

From the Bayesian model we calculated dust accumulation rates (DAR, cm/ka) for the period from ~100 to ~40 ka (Fig. 4). We decided to not include data from <150 cm so that we are not affected by possible effects of pedogenic or colluvial disturbances on the $pIRIR_{200,290}$ ages of PC0.

5. Discussion

5.1. *Field observations versus luminescence age model*

Here we discuss the stratigraphy recorded in the field (including suspected hiatuses) and the measured magnetic susceptibility (MS) considering the newly obtained luminescence ages ($pIRIR_{200,290}$ ages only, Fig. 3).

The upper 16 m of the section are represented by an upper heavily eroded soil of presumed Holocene age (PC0), a thick L1 loess unit and two distinct palaeosols forming PC 1. The structure of the pedocomplex corresponds to the regional appearance of PC 1 (Tokareva et al., 2023), which has been assigned to MIS 5 (Dodonov, 2002). The sharpness in the transition of MS values from loess L1 to PC 1 at a depth of 11.5 m may indicate the absence of the upper part of the pedocomplex – the top part of the soil of the MIS 5a substage. Field descriptions and the MS curve suggest the presence of a hiatus at the base of PC1, since this regionally developed pedocomplex consists of 3 developed palaeosols, the

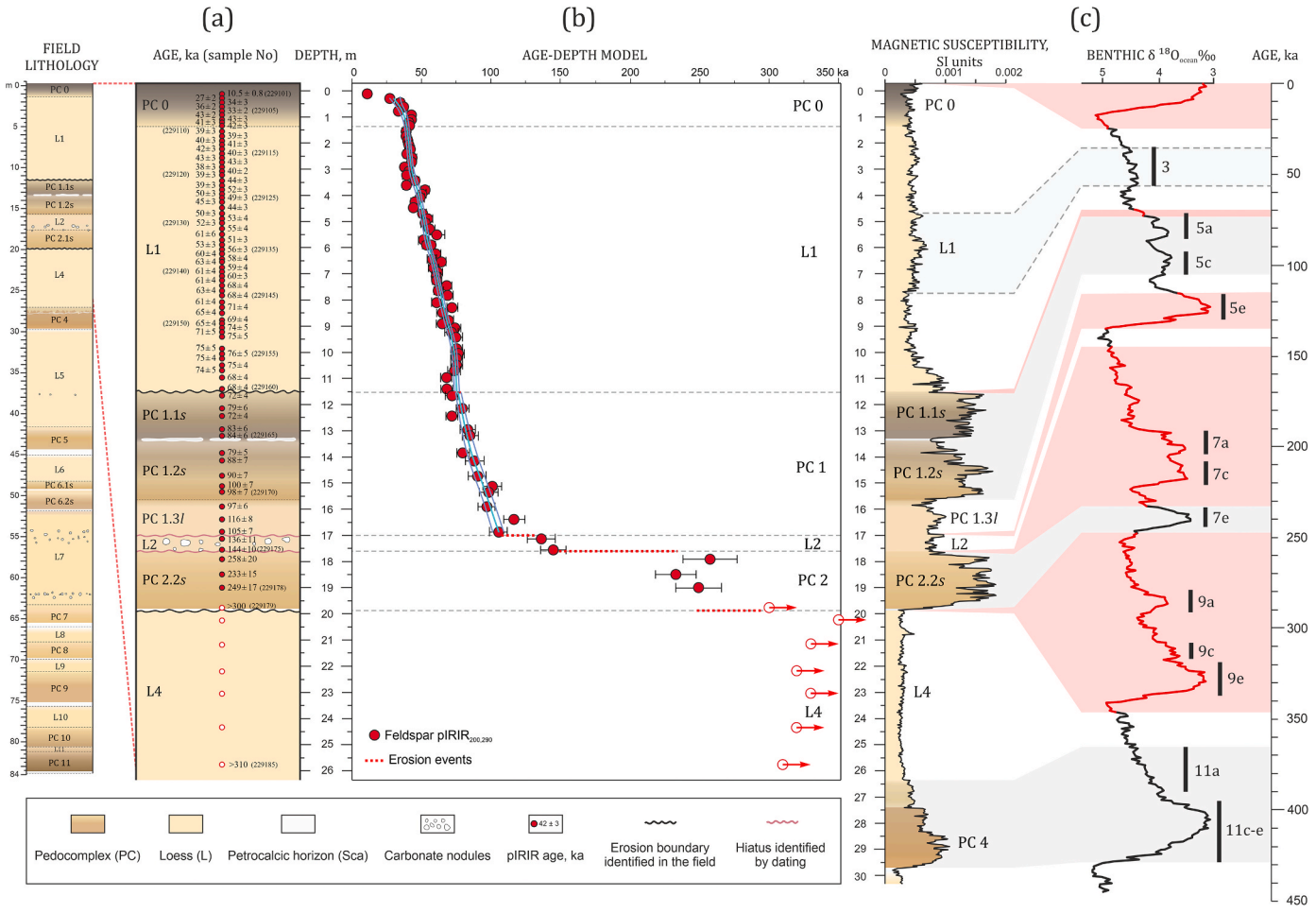

Fig. 3. A) Stratigraphy, b) $pIRIR_{200,290}$ chronology (incl. Bayesian model), c) magnetic susceptibility and correlation with the MIS record (Railsback et al., 2015) for the Kuldara section.

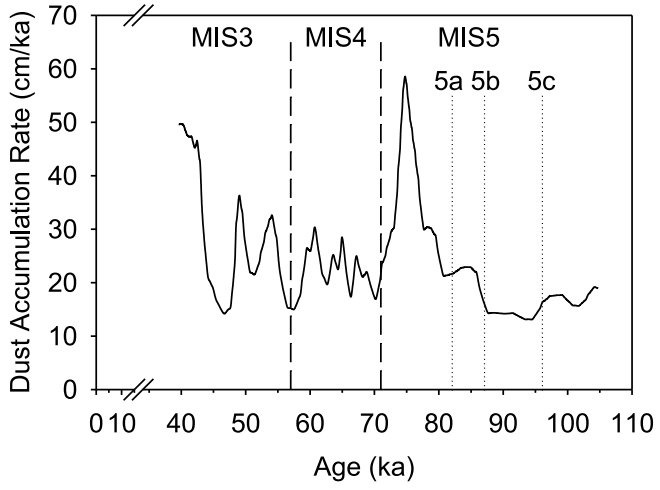

Fig. 4. Dust accumulation rate at Kuldara during the Late Pleistocene.

lowermost always being the thickest and most developed, with characteristic dark gray colour. Another feature of this soil (PC1.3s in Khovaling chart) is a very pronounced peak in the magnetic susceptibility (Tokareva et al., 2023, 2024; Dodonov, 2002). At Kuldara we see only two equally developed soils in PC1 with similar MS values. Thus, field observations lead to a hypothesis that the PC1.3s palaeosol, corresponding to the MIS 5e stage, is absent from the sequence and that a part of the top of PC1 is missing. The luminescence chronology clearly shows that PC0 is not of Holocene age, the loess at the base of the PC0 is dated to ~40 ka. A significant part of the section is missing (Holocene soil and the upper part of L1 corresponding to last 10 ka of MIS3, entire MIS2 and MIS1). It also seems that the suspected hiatus at 11.5 m, if present at all, must be quite small (few ka) because the luminescence ages do not show any sign of an age gap over this interval. It must be noted that random uncertainties on the luminescence ages at 11.5 m are of the order of 1.5–2 ka so a hiatus must be significantly larger than this to be detectable. The luminescence ages confirm the missing PC1.3s soil (MIS5e) as evidenced by an 'age jump' from ~110 ka to ~130 ka at a depth of 17 m (between samples 229173 and 74).

The interval between 16 and 20 m has a complex structure. The loess unit L2 has a thickness of 2.3 m, which is significantly less than in other sections of the Khovaling Loess Plateau. At the Khonako-III outcrop, L2 loess has an average thickness of ~8 m, reaching a maximum thickness of 12 m in the Khonako-II section (Dodonov, 2002). However, at the Obi-Mazar outcrop adjacent to Kuldara, L2 also has a smaller thickness - about 3.5 m (Tokareva et al., 2023). Despite the fact that no visible unconformities were found in the description of the section, the low thickness of the unit may indicate active erosion events during MIS 6. The second pedocomplex (PC2) is represented by one developed palaeosol with a thickness of 2.25 m. However, similar to PC1 above, in the Khovaling area PC2 is usually formed by two developed palaeosols with a pronounced interlayer of loess affected by pedogenesis which has

a characteristic olive colour (Dodonov, 2002). The characteristic features of this PC (dark brown colour, structure, powerful MS peak) suggest that it should be correlated with the upper part of PC 2 of Khovaling LPS (Tokareva et al., 2024), and, accordingly, with MIS7a-c. At the base of the palaeosol at a depth of 19.8 m we found a pronounced erosional boundary - a sharp transition into the underlying loess unit. The luminescence chronology shows the presence of a significant hiatus of ~110 ka in duration at a depth of 17.5 m which was not identifiable in the field. In addition, the luminescence ages of PC2 show that the palaeosol can be correlated to MIS7e (and not to MIS7a-c as presumed from field and magnetic data).

The unit located below 19.8 m is represented by typical loess with a thickness of 7.2 m and was correlated in the field with the L4 horizon of the regional LPS scheme. The underlying pedocomplex in the interval of 27–30 m is represented by a developed palaeosol with a characteristic dark brown colour, but with MC values two times lower than the overlying palaeosols (Fig. 3c). The structural features of this PC, its thickness, the presence of a carbonate crust at the base and archaeological artefacts (Kulakova et al., 2024) allow us to correlate this pedocomplex with PC 4 of the regional scheme. Thus, in the upper part of the Kuldara section field observations suggest that we lack PC 3. This conclusion is supported by the fact that, firstly, in the neighbouring Obi-Mazar outcrop the third PC (PC3) comprises three palaeosols, two distinct MS peaks with values of the order of MS peaks for PCs 1 and 2, two carbonate crusts, and a complete absence of archaeological finds (Ranov and Karimova, 2005). Based on these findings, we correlate L4 with MIS 10, and PC 4 with MIS 11. The minimum age (>300 ka) for sample 229,179 confirms indeed an erosional boundary at a depth of 19.8 m and a hiatus of a least 60 ka. The sample with the lowest dose rate in the series 229179 to −85 gives a minimum age of >340 ka, which would increase the hiatus to ~100 ka and place the loess layer below clearly into MIS10. Thus, luminescence confirms the field observations and correlations with nearby sections that L3 and PC3 are missing.

5.2. Dust accumulation at kuldara

Fig. 4 shows the dust accumulation rate (DAR) plotted against an independent luminescence time scale. The MIS5/4 (71ka) and MIS4/3 (57 ka) boundaries and ages of MIS5 peaks (a,b,c) are also shown as vertical dashed and dotted lines, respectively. Small dust peaks may correlate with the warmer phases in MIS5 (a and c). A massive increase in dust from ~20 cm/ka to ~60 cm/ka occurs towards the end of MIS5 when climate moves towards more glacial conditions. During MIS4, three minor dust peaks can be distinguished at ~68, ~65 and ~61 ka. As climatic conditions improved a little during MIS3, we observe again high dust accumulation peaks at ~54, ~49 and ~40 ka; especially the dust peak at ~40 ka is very pronounced. It is interesting to note that during the MIS4-3 glacial period the dust peaks systematically increase in amplitude as the climatic conditions ameliorated.

Future comparisons with data from sections closeby (Khonako, Obi Mazar) in the Khovaling Loess Plateau should allow us to extend the DAR data in time and confirm whether or not the dust peaks we observe at Kuldara are influenced by local site factors or whether they are a more regional phenomenon.

6. Conclusions

The post-IR_{200} $IRSL_{290}$ luminescence characteristics of coarse-silt polymineral grains are satisfactory (reproducible growth and satisfactory dose recovery) and finite luminescence ages back to ~250 ka were obtained; for older samples we report minimum ages of >300 ka (equivalent to 92% of saturation, 2.5xD_c). The luminescence chronology reveals several erosional hiatuses in the sequence: 1) the upper L1 (MIS2) and Holocene units are missing; 2) the MIS5e soil (PC1.3s) is missing; 3) most part of MIS6 (L2) and the entire MIS7a,c soil (PC2.1s) have been deflated; and 4) the loess and palaeosol units of MIS8 and 9 (L3 and PC3, respectively) are absent. Our luminescence chronology confirms one erosional boundary detected in the field but also reveals the presence of two new deflation surfaces that were not visible during field observations. Dust Accumulation Rates (DAR) for the Late Pleistocene show, next to several minor peaks, two major dust accumulation peaks, one at ~75 ka (end of MIS5) and one at ~40 ka (MIS3b). We conclude that sedimentological field data (including field magnetic susceptibility) in combination with high-resolution luminescence chronologies are necessary to fully unravel the chronostratigraphy of the upper part of the loess-palaeosol sequence at Kuldara.

CRediT authorship contribution statement

J.-P. Buylaert: Conceptualization, Data curation, Formal analysis, Funding acquisition, Investigation, Methodology, Project administration, Resources, Supervision, Validation, Visualization, Writing – original draft, Writing – review & editing. **A. Challier:** Data curation, Formal analysis, Investigation, Methodology, Project administration. **E. P. Kulakova:** Data curation, Formal analysis, Investigation, Methodology, Resources, Writing – original draft, Writing – review & editing. **N. A. Taratunina:** Data curation, Formal analysis, Investigation, Methodology, Resources. **K.J. Thomsen:** Data curation, Formal analysis, Investigation, Methodology, Supervision. **A.O. Utkina:** Investigation, Methodology, Resources. **P.M. Sosin:** Conceptualization, Funding acquisition, Investigation, Methodology, Resources, Supervision. **O.A. Tokareva:** Data curation, Formal analysis, Investigation, Resources. **A. A. Anoikin:** Conceptualization, Funding acquisition, Investigation, Resources. **T.U. Khujageldiev:** Conceptualization, Data curation, Formal analysis, Investigation, Methodology, Resources, Writing – review & editing. **C. Karayev A:** Data curation, Investigation, Methodology, Resources. **N.K. Ubaydulloev:** Funding acquisition. **A.S. Murray:** Conceptualization, Funding acquisition, Methodology. **R.N. Kurbanov:** Conceptualization, Funding acquisition, Investigation, Methodology, Project administration, Resources, Supervision, Validation, Writing – original draft, Writing – review & editing.

Declaration of competing interest

The authors declare the following financial interests/personal relationships which may be considered as potential competing interests: Jan-Pieter Buylaert reports financial support was provided by Nordic Council of Ministers. If there are other authors, they declare that they have no known competing financial interests or personal relationships that could have appeared to influence the work reported in this paper.

Data availability

Data will be made available on request.

Acknowledgements

This work was partly supported by NordForsk through the funding to ‘The timing and ecology of the human occupation of Central Asia, project number 105204’. We thank our THOCA colleagues for their continuous support in the field and the laboratory since the start of our field excavations at Kuldara site in spring 2021.

Appendix A. Supplementary data

Supplementary data to this article can be found online at https://doi.org/10.1016/j.quageo.2024.101545.

References

Anoikin, A., Sosin, P., Rybalko, A., Khudjageldiev, T., Sharipov, A., Karayev, A., Kulakova, E., Meshcheryakova, O., Tokareva, O., Kurbanov, R., 2023a. Lakhuti-IV –

a new site of the early palaeolithic in central Asia (Tajikistan). Archaeological Research in Asia 35, 100466. https://doi.org/10.1016/j.ara.2023.100466.
Aitken, M.J., 1985. Thermoluminescence Dating. Academic Press, London.
Anoikin, A.A., Rybalko, A.G., Khudjageldiev, T.U., Sosin, P.M., Sharipov, A.F., Kurbanov, R.N., 2023b. Lakhuti-IV: a new site of the loessic paleolithic in Tajikistan. Archaeol. Ethnol. Anthropol. Eurasia 51 (2), 3–13.
Autzen, M., Andersen, C.E., Bailey, M., Murray, A.S., 2022. Calibration quartz: an update on dose calculations for luminescence dating. Radiat. Meas. 157, 106828 https://doi.org/10.1016/j.radmeas.2022.106828.
Blaauw, M., Christen, J.A., 2011. Flexible palaeoclimate age-depth models using an autoregressive gamma process. Bayesian Analysis 6, 457–474. https://doi.org/10.1214/11-BA618.
Banerjee, D., Murray, A.S., Bøtter-Jensen, L., Lang, A., 2001. Equivalent dose estimation using a single aliquot of polymineral fine grains. Radiat. Meas. 33, 73–94. https://doi.org/10.1016/S1350-4487(00)00101-3.
Bøtter-Jensen, L., Andersen, C.E., Duller, G.A.T., Murray, A.S., 2003. Developments in radiation, stimulation and observation facilities in luminescence measurements. Radiat. Meas. 37, 535–541. https://doi.org/10.1016/S1350-4487(03)00020-9.
Buylaert, J.P., Vandenberghe, D., Murray, A.S., Huot, S., De Corte, F., Van den Haute, P., 2007. Luminescence dating of old (>70ka) Chinese loess: a comparison of single-aliquot OSL and IRSL techniques. Quat. Geochronol. 2, 9–14. https://doi.org/10.1016/j.quageo.2006.05.028.
Buylaert, J.-P., Jain, M., Murray, A.S., Thomsen, K.J., Thiel, C., Sohbati, R., 2012. A robust feldspar luminescence dating method for Middle and Late Pleistocene sediments. Boreas 41, 435–451.
Challier, A., Thomsen, K.J., Kurbanov, R., Sosin, P., Murray, A., Guérin, G., Meshcheryakova, O., Karayev, A., Khormali, F., Taratunina, N., Utkina, A., Buylaert, J.-P. A detailed quartz and feldspar luminescence chronology for the Khonako II loess section (South Tajikistan). Submitted to Quaternary Geochronology, LED2023 proceedings..
Chapot, M.S., Roberts, H.M., Duller, G.A.T., Lai, Z.P., 2012. A comparison of natural- and laboratory-generated dose response curves for quartz optically stimulated luminescence signals from Chinese Loess. Radiat. Meas. 47, 1045–1052. https://doi.org/10.1016/j.radmeas.2012.09.001.
Cresswell, A.J., Carter, J., Sanderson, D.C.W., 2018. Dose rate conversion parameters: assessment of nuclear data. Radiat. Meas. 120, 195–201. https://doi.org/10.1016/j.radmeas.2018.02.007.
Cunningham, A.C., Wallinga, J., 2010. Selection of integration time intervals for quartz OSL decay curves. Quat. Geochronol. 5, 657–666. https://doi.org/10.1016/j.quageo.2010.08.004.
Ding, Z.L., Ranov, V., Yang, S.L., Finaev, A., Han, J.M., Wang, G.A., 2002. The loess record in southern Tajikistan and correlation with Chinese loess. Earth Planet Sci. Lett. 200, 387–400. https://doi.org/10.1016/S0012-821X(02)00637-4.
Dodonov, A.E., 2002. Quaternary Period of Central Asia: Stratigraphy, Correlation, Paleogeography. GEOS, Moscow, p. 250 (In Russ.).
Dodonov, A.E., 2007. Loess records | central Asia. In: Elias, S.A. (Ed.), Encyclopedia of Quaternary Science. Elsevier Ltd, London, pp. 1418–1429.
Duller, G.A.T., 2015. The Analyst software package for luminescence data: overview and recent improvements. Ancient TL 33, 35–42.
Frechen, M., Dodonov, A.E., 1998. Loess chronology of the Middle and upper Pleistocene in tadjikistan. Int. J. Earth Sci. 87, 2–20. https://doi.org/10.1007/s005310050185.
Hansen, V., Murray, A., Thomsen, K., Jain, M., Autzen, M., Buylaert, J.-P., 2018. Towards the origins of over-dispersion in beta source calibration. Radiat. Meas. 120, 157–162. https://doi.org/10.1016/j.radmeas.2018.05.014.
Huntley, D.J., Baril, M.R., 1997. The K content of the K-feldspars being measured in optical dating or in thermoluminescence dating. Ancient Tl 15, 11–13.
Huntley, D.J., Hancock, R.G.V., 2001. The Rb contents of the K-feldspar grains being measured in optical dating. Ancient TL 19, 43–46.
Kulakova, E.P., Anoikin, A.A., Khudzhageldiev, T.U., Sosin, P.M., Tokareva, O.A., Karaev, A.Ch, Rybalko, A.G., Kurbanov, R.N., 2024. Stratigraphy and geochronology of the early paleolithic site of Kuldara (Tajikistan). Geomorphology and Palaeogeography (in press). (In Russ.).
Kulakova, E.P., Kurbanov, R.N., 2023. First paleomagnetic data on the Matuyama-Brunhes transition in the loess-paleosol series of Tajikistan. In: Kosterov, A., Lyskova, E., Mironova, I., Apatenkov, S., Baranov, S. (Eds.), Problems of Geocosmos–2022. Springer Proceedings in Earth and Environmental Sciences. Springer, Cham, pp. 67–84. https://doi.org/10.1007/978-3-031-40728-4_6.
Lai, Z.P., Zöller, L., Fuchs, M., Brückner, H., 2008. Alpha efficiency determination for OSL of quartz extracted from Chinese loess. Radiat. Meas. 43, 767–770. https://doi.org/10.1016/j.radmeas.2008.01.022.
Lapp, T., Kook, M., Murray, A.S., Thomsen, K.J., Buylaert, J.-P., Jain, M., 2015. A new luminescence detection and stimulation head for the Risø TL/OSL reader. Radiat. Meas. 81, 178–184. https://doi.org/10.1016/j.radmeas.2015.02.001.
Li, B., Li, S.-H., 2011. Luminescence dating of K-feldspar from sediments: a protocol without anomalous fading correction. Quat. Geochronol. 6, 468–479. https://doi.org/10.1016/j.quageo.2011.05.001.
Li, B., Li, S., 2012. A reply to the comments by Thomsen et al. on "Luminescence dating of K-feldspar from sediments: a protocol without anomalous fading correction.". Quat. Geochronol. 8, 49–51. https://doi.org/10.1016/j.quageo.2011.10.001.
Martin, L., Mercier, N., Incerti, S., 2014. Geant4 simulations for sedimentary grains in infinite matrix conditions: the case of alpha dosimetry. Radiat. Meas. 70, 39–47. https://doi.org/10.1016/j.radmeas.2014.09.003.
Mejdahl, V., Bøtter-Jensen, L., 1994. Luminescence dating of archaeological materials using a new technique based on single aliquot measurements. Quat. Sci. Rev. 13, 551–554. https://doi.org/10.1016/0277-3791(94)90076-0.
Murray, A.S., Marten, R., Johnston, A., Martin, P., 1987. Analysis for naturally occurring radionuclides at environmental concentrations by gamma spectrometry. J. Radioanal. Nucl. Chem. 115, 263–288. https://doi.org/10.1007/BF02037443.
Murray, A.S., Wintle, A.G., 2003. The single aliquot regenerative dose protocol: potential for improvements in reliability. Radiat. Meas. 37, 377–381. https://doi.org/10.1016/S1350-4487(03)00053-2.
Murray, A.S., Helsted, L.M., Autzen, M., Jain, M., Buylaert, J.P., 2018. Measurement of natural radioactivity: calibration and performance of a high-resolution gamma spectrometry facility. Radiat. Meas. 120, 215–220. https://doi.org/10.1016/j.radmeas.2018.04.006.
Murray, A.S., Schmidt, E.D., Stevens, T., Buylaert, J.-P., Marković, S.B., Tsukamoto, S., Frechen, M., 2014. Dating Middle Pleistocene loess from Stari Slankamen (Vojvodina, Serbia) — Limitations imposed by the saturation behaviour of an elevated temperature IRSL signal. CATENA, Loess and dust dynamics, environments, landforms, and pedogenesis: a tribute to Edward Derbyshire 117, 34–42. https://doi.org/10.1016/j.catena.2013.06.029.
Murray, A.S., Arnold, L.J., Buylaert, J.-P., Guérin, G., Qin, J., Singhvi, A.K., Smedley, R., Thomsen, K.J., 2021. Optically stimulated luminescence dating using quartz. Nat Rev Methods Primers 1, 72. https://doi.org/10.1038/s43586-021-00068-5.
Parviz, N., Shen, Z., Yunus, M., Zulqarnain, S., 2020. Loess deposits in southern Tajikistan (Central Asia): Magnetic properties and paleoclimate. Quaternary Geochronology 60, 101114. https://doi.org/10.1016/j.quageo.2020.101114.
Prescott, J.R., Hutton, J.T., 1994. Cosmic ray contributions to dose rates for luminescence and ESR dating: large depths and long-term time variations. Radiat. Meas. 23, 497–500. https://doi.org/10.1016/1350-4487(94)90086-8.
Railsback, L.B., Gibbard, P.L., Head, M.J., Voarintsoa, N.G., Toucanne, S., 2015. An optimized scheme of lettered marine isotope substages for the last 1.0 million years, and the climatostratigraphic nature of isotope stages and substages. Quat. Sci. Rev. 111, 94–106. https://doi.org/10.1016/j.quascirev.2015.01.012.
Ranov, V., 1995. The 'loessic palaeolithic' in South Tadjikistan, Central Asia: its industries, chronology and correlation. Quat. Sci. Rev. 14, 731–745. https://doi.org/10.1016/0277-3791(95)00055-0.
Ranov, V.A., Dodonov, A.E., Lomov, S.P., Pakhomov, M.M., Penkov, A.V., 1987. Kuldara – a new early palaeolithic site in southern Tajikistan. Bulletin of the Commission for Study of the Quaternary of the Academy of Sciences of the USSR 56, 65–75 (In Russ.).
Ranov, V.A., Karimova, G.R., 2005. Stone Age of the Afghan-Tajik Depression. Devashtich, Dushanbe, p. 252 (In Russ.).
Ranov, V.A., Schaefer, J., 2000. Loess Palaeolithic. Archeology, Ethnography and Anthropology of Eurasia, vol. 2, pp. 20–32 (In Russ.).
Schäfer, J., Ranov, V.A., Sosin, P., 1998. The cultural evolution of man and the chronostratigraphical background of changing environments in the loess palaeosoil sequences of Obi-Mazar and Khonako (Tajikistan). Anthropologie 36, 121–135.
Schmidt, C., Bösken, J., Kolb, T., 2018. Is there a common alpha-efficiency in polymineral samples measured by various infrared stimulated luminescence protocols? Geochronometria 45, 160–172. https://doi.org/10.1515/geochr-2015-0095.
Sohbati, R., Murray, A., Lindvold, L.R., Buylaert, J.-P., Jain, M., 2017. Optimization of laboratory illumination in optical dating. Quat. Geochronol. 39, 105–111. https://doi.org/10.1016/j.quageo.2017.02.010.
Stevens, T., Buylaert, J.-P., Thiel, C., Újvári, G., Yi, S., Murray, A.S., Frechen, M., Lu, H., 2018. Ice-volume-forced erosion of the Chinese Loess Plateau global Quaternary stratotype site. Nat. Commun. 9, 983. https://doi.org/10.1038/s41467-018-03329-2.
Thiel, C., Horváth, E., Frechen, M., 2014. Revisiting the loess/palaeosol sequence in Paks, Hungary: a post-IR IRSL based chronology for the 'Young Loess Series'. Quat. Int. 319, 88–98. https://doi.org/10.1016/j.quaint.2013.05.045.
Timar-Gabor, A., Wintle, A.G., 2013. On natural and laboratory generated dose response curves for quartz of different grain sizes from Romanian loess. Quat. Geochronol. 18, 34–40. https://doi.org/10.1016/j.quageo.2013.08.001.
Tokareva, O.A., Lebedeva, M.P., Sosin, P.M., Ashurmadov, I.K., Kurbanov, R.N., 2023. Structures and properties of paleosols of the Late Pleistocene of the loess-soil section of Obi-Mazar (Tajikistan). Izvestiya Rossiiskoi Akademii Nauk. Seriya Geograficheskaya (in press). (In Russ.).
Tokareva, O.A., Lebedeva, M.P., Sosin, P.M., Ashurmadov, I.K., Khormali, F., Kurbanov, R.N., 2024. Structure and properties of paleosols of the last two interglacial cycles of the Khovaling Loess Plateau, Tajikistan (section of Obi-Mazar). Quaternary Research. (in press).
Vandenberghe, D., De Corte, F., Buylaert, J.-P., Kučera, J., Van den haute, P., 2008. On the internal radioactivity in quartz. Radiat. Meas. 43, 771–775. https://doi.org/10.1016/j.radmeas.2008.01.016.
Volvakh, N.E., Kurbanov, R.N., Zykina, V.S., Murray, A.S., Stevens, T., Költringer, C.A., Volvakh, A.O., Malikov, D.G., Taratunina, N.A., Buylaert, J.-P., 2022. First high-resolution luminescence dating of loess in Western Siberia. Quat. Geochronol. 73, 101377 https://doi.org/10.1016/j.quageo.2022.101377.
Wintle, A.G., Murray, A.S., 2006. A review of quartz optically stimulated luminescence characteristics and their relevance in single-aliquot regeneration dating protocols. Radiat. Meas. 41, 369–391. https://doi.org/10.1016/j.radmeas.2005.11.001.
Yi, S., Buylaert, J.-P., Murray, A.S., Lu, H., Thiel, C., Zeng, L., 2016. A detailed post-IR IRSL dating study of the Niuyangzigou loess site in northeastern China. Boreas 45, 644–657. https://doi.org/10.1111/bor.12185.
Zhao, H., Li, S., 2005. Internal dose rate to K-feldspar grains from radioactive elements other than potassium. Radiat. Meas. 40, 84–93.